PHYSICAL REVIEW B VOLUME 39, NUMBER 1 1 JANUARY 1989

Elastic electron backscattering from surfaces

A. Jablonski and J. Gryko
Institute of Physical Chemistry, Polish Academy of Sciences, ul. Kasprzaka 44/52, 01-224 Warszawa, Poland

J. Kraaer and S. Tougaard
Fysisk Institut, Odense Universitet, DK-5230 Odense M, Denmark
(Received 21 March 1988; revised manuscript received 15 August 1988)

Elastic electron backscattering from solid surfaces has been studied experimentally and theoretically. It has been shown that the recently published P_1 approximation gives an inadequate description. Much more realistic results are obtained from the Monte Carlo algorithm based on differential cross sections calculated within the partial-wave expansion method. Excellent agreement has been found between the calculated results and the experimental data obtained in the present work or taken from the literature. The present calculations seem to be valid for electron energies exceeding 200 eV and for low- and medium-atomic-number elements. The possibility of measuring the inelastic mean free path of electrons from the elastically backscattered intensity is discussed.

I. INTRODUCTION

The problem of elastic electron backscattering has been gaining attention over the past several years. This phenomenon is the physical basis of some surface-sensitive electron spectroscopies, e.g., low-energy electron diffraction (LEED). The so-called elastic peak corresponding to elastically backscattered electrons is frequently monitored in quantitative Auger spectroscopy for positioning the sample. Elastically backscattered electrons contribute also in the signal recorded in high-energy electron appearance potential spectroscopy (HEAPS).[1] The experimental techniques involving quantitative estimation of the elastic peak intensity were given the common name of elastic peak electron spectroscopy (EPES).[2,3] An important application of EPES is the determination of the inelastic mean free path (IMFP) of electrons in solids.[4] Unexpectedly, there are only a few experimental studies of elastic electron backscattering published in the literature for energies used in surface electron spectroscopies (50–3000 eV).[5–10] The elastic backscattering phenomenon can be quantitatively described by the angular distribution of reflected electrons and by the probability of elastic reflection (reflection coefficient).

These parameters were measured in several experimental studies at relatively low electron energies.[5–7] Schilling and Webb[5] published the angular distribution of electrons elastically backscattered from liquid mercury at energies below 500 eV. Similar measurements made for a number of polycrystalline elements at energies below 200 eV were recently reported by Oguri *et al.*[7] Most extensive data on angular distribution of electrons backscattered from polycrystalline films in the energy range 100–2000 eV were published by Bronshtein *et al.*[8] and Bronshtein and Pronin.[9] It has been found that the shape of the angular distribution can be very involved, exhibiting minima and maxima, particularly for medium- and high-atomic-number elements. Schmid *et al.*[10] published values, for energies up to 2500 eV, of the reflection coefficient measured within the solid angle of the retarding field analyzer. These dependences were also found to be rather involved. A number of values of the reflection coefficient were estimated by Gergely.[2]

In view of the wide application of the elastic backscattering effect in electron spectroscopies there is an obvious need for a theoretical description of this phenomenon. Several theoretical approaches were published in the literature.[4,5,11] Within the simplest approach it is assumed that the electron leaving the solid undergoes only one large angle elastic scattering (single elastic scattering model).[4] More realistic are the theoretical models assuming multiple elastic scattering of electrons in the solid.[4,5,11] Some of the applications of EPES, particularly the determination of IMFP, require an accurate theoretical description of elastic backscattering. However, to the knowledge of the authors, a critical comparison of all existing theories and the experimental data has never been made. It has therefore been decided to design a simple experimental method for determining the relative intensities of reflected electrons. The other objective of the present paper is to perform extensive calculations and to compare the theoretical results with experimental data recorded in the present work and those already published in the literature.

II. THEORY

A. Analytical description of multiple elastic scattering

An extensive theoretical treatment of the elastic electron transport in a solid in the forward direction was published by Goudsmit and Saunderson as early as 1940.[12] This multiple elastic scattering theory was applicable for high energies. Theoretical analysis of multi-

 ©1989 The American Physical Society

ple elastic scattering in solids has received surprisingly little attention at energies relevant for surface electron spectroscopies. Schilling and Webb[5] proposed an analytical expression describing well the elastic backscattering of electrons from liquid mercury in the energy range 100–500 eV. The theoretical description of electron transport in solids was also analyzed in a recent paper by Tofterup.[11] The validity of this theory in the range of the elastic peak will be discussed in the present paper. For this reason, let us first briefly summarize main features of this approach.

Let the solid surface be bombarded with a monoenergetic flux $F(E)=\delta(E-E_0)$ of electrons. Then the energy and angular distribution of the flux of backscattered electrons is given by[11]

$$J_1(E,\mathbf{\Omega})=\int Q(E_0,\mathbf{\Omega}_0,x=0;R,\mathbf{\Omega})G(E_0,R;E)dR \ ,$$

where $Q(E_0,\mathbf{\Omega}_0,x;R,\mathbf{\Omega})dR\,d\Omega^2$ is the probability for an electron with initial energy E_0 and direction $\mathbf{\Omega}_0$ to pass a plane at depth x in direction $(\mathbf{\Omega},d^2\Omega)$ after having traveled a path length R in the solid. $G(E_0,R;E)$ is the probability that an electron with initial energy E_0 has energy E after having traveled the path length R in the solid. Let α_0 and α denote the incidence and exit angles both with respect to the outgoing surface normal. Within the P_1 approximation to the Boltzmann transport equation Tofterup found that[11]

$$Q(E_0,\eta_0,x=0;R,\eta)=\frac{2\sqrt{3}}{\pi}\left[1+\frac{1}{2\eta_0}\right](\tfrac{3}{2}\eta^2+\eta)\lambda_1^{-1} \times\int_0^1 e^{-uR/\lambda_1}\frac{\sqrt{u(1-u)}}{u+3}du \ ,$$

where λ_1 is the transport mean free path for elastic electron scattering, $\eta=\cos\alpha$, $\eta_0=\cos\alpha_0$ and the direction of positive flux is outwards. Note the difference in notation in comparison with Ref. 11. Finally, the flux of elastically backscattered electrons is given by[11]

$$J_1(E,\eta)=\frac{\sqrt{3}}{(2+\sqrt{3})^2}\left[1+\frac{1}{2\eta_0}\right](\tfrac{3}{2}\eta^2+\eta)\frac{1}{A+\lambda_1/\lambda} \times[\delta(E-E_0)+\cdots] \ , \quad (1)$$

where λ is the electron inelastic mean free path and $A\cong 0.42$.

Equation (1) predicts the angular distribution to be given by the simple expression $\frac{3}{2}\eta^2+\eta$, which in view of the reported experimental results,[8,9] does not seem to be realistic. Actually, the P_1 approximation is expected to be insufficient when the typical electron contributing to the spectrum has undergone few elastic scattering events.[11] However, it has been argued that the P_1 approximation may apply even for small path lengths for the heavy elements but is expected to be less accurate for the light elements.[11] To establish the limits of validity of the P_1 approximation we have decided to compare Eq. (1) with the experimental intensities of elastically backscattered electrons and also with other theoretical models.

B. Monte Carlo simulation of multiple elastic scattering

As an alternative approach, the Monte Carlo algorithms have been extensively used in describing the medium-energy electron transport in solids.[4,13,14] The electron trajectory is usually assumed to follow the Poisson stochastic process.[15,16] The linear path lengths Δx between successive elastic collisions are then described by the exponential distribution

$$f(\Delta x)=(1/\lambda_\theta)\exp(-\Delta x/\lambda_\theta) \ ,$$

with the mean value λ_θ equal to the elastic mean free path

$$\lambda_\theta=(N\sigma_t)^{-1} \ ,$$

where σ_t is the total elastic scattering cross section and N is the atomic density. The elastic scattering event is described by the polar and azimuthal angles after collision. Taking advantage of cylindrical symmetry of the scattering process by the central field potential we can assume that azimuthal angles follow the uniform distribution. However, major numerical difficulties are associated with simulating the distribution of polar scattering angles. The corresponding probability density function is given by[4]

$$W(\theta)=(d\sigma/d\theta)/\sigma_t \ ,$$

where $d\sigma/d\theta$ is the differential elastic scattering cross section. Ichimura *et al.*[13] has shown that at energies relevant for surface electron spectroscopies the scattering cross sections cannot be calculated within the first-order Born approximation. The partial-wave analysis is necessary for an accurate description of the scattering event. Finally, the probability of inelastic collisions along the trajectory of a given electron was accounted by the factor $\exp(-x/\lambda)$, where x is the trajectory length.

Monte Carlo simulation of the electron elastic backscattering requires a considerable amount of computer time. The probability of the electron elastic backscattering from surfaces is relatively small, particularly for low-atomic-number elements.[2–10] As a consequence, a considerable number of complete electron trajectories has to be followed to obtain reasonable statistics. In the present work the total number of trajectories varied between 200 000 and 500 000. In effect, the statistical error of the total elastically backscattered current was close to $\sim 1\%$. The Monte Carlo scheme used in the present work has been described in detail elsewhere.[4] Instead of the first-order Born approximation,[4] in the present algorithm the partial-wave expansion method was used to calculate the elastic scattering cross sections. A number of data on the elastic scattering cross section was published in the literature.[17–21] However, these data were compiled for selected energies and elements. For this reason it has been decided in the present work to develop general algorithms making calculations of the differential elastic scattering cross sections possible for any electron energy and any element. Details of these calculations are given in the following sections.

A similar Monte Carlo scheme was extensively used by Ichimura *et al.*[13] and by Ichimura and Shimizu.[14] How-

ever, their algorithm simulated also the energy losses along the electron trajectory. These authors calculated mainly the energy distribution of backscattered electrons, and eventually the backscattering correction in quantitative Auger electron spectroscopy.

C. Nonrelativistic approach

The wave function describing the elastically scattered electron can be expressed by a series of functions $u_l(r)$ satisfying the following equation:[22]

$$\frac{d^2u_l}{dr^2}+\left[K^2-\frac{l(l+1)}{r^2}-\frac{2m}{\hbar^2}V(r)\right]u_l=0 , \tag{2}$$

with the boundary conditions

$$u_l(0)=0 ,$$

$$u_l(Kr)\rightarrow\sin(Kr-l\pi/2+\delta_l) \text{ as } r\rightarrow\infty ,$$

where $K=(2mE/\hbar^2)^{1/2}$ and all other symbols have their usual meaning. The differential scattering cross section corresponding to a given electron-atom interaction potential $V(r)$ can be expressed in terms of the phase shifts δ_l only:[23]

$$d\sigma/d\Omega=A^2+B^2 , \tag{3}$$

where

$$A=\frac{1}{2K}\sum_{l=0}^{\infty}(2l+1)(\cos2\delta_l-1)P_l(\cos\theta) ,$$

$$B=\frac{1}{2K}\sum_{l=0}^{\infty}(2l+1)\sin2\delta_l P_l(\cos\theta) .$$

One of the possible methods for calculating the phase shifts was proposed by Calogero.[24] The following expression is substituted into Eq. (2):

$$\frac{u_l'}{u_l}=K\frac{\cos\delta_l(r)\hat{j}_l'(Kr)-\sin\delta_l(r)\hat{n}_l'(Kr)}{\cos\delta_l(r)\hat{j}_l(Kr)-\sin\delta_l(r)\hat{n}_l(Kr)} ,$$

where $\hat{j}_l(x)$ and $\hat{n}_l(x)$ are the linearly independent solutions of the Riccatti-Bessel equation, and $\delta_l(r)$ is the phase function. After extensive derivation the following first-order differential equation is obtained:

$$\delta_l'(r)=-\frac{1}{K}\frac{2m}{\hbar^2}V(r)[\hat{j}_l(Kr)\cos\delta_l(r)-\hat{n}_l(Kr)\sin\delta_l(r)]^2 , \tag{4}$$

with the initial condition $\delta_l(0)=0$. The phase shifts are determined from the asymptotic behavior of the phase function

$$\lim_{r\rightarrow\infty}\delta_l(r)=\delta_l .$$

The right-hand side of Eq. (4) cannot be calculated at $r=0$. Thus, the numerical integration of Eq. (4) should be started from a different boundary condition. It can be proved that (see Appendix)

$$\hat{j}_l(Kr)\cos\delta_l(r)\gg\hat{n}_l(Kr)\sin\delta_l(r)$$

for small values of r. A new boundary condition can be estimated from

$$\tan\delta_l(r)\simeq\delta_l(r)=-\frac{1}{K}\frac{2m}{\hbar^2}\int_0^r V(r')\hat{j}_l^2(Kr')dr' .$$

In the present work the scattering centers of the solid were approximated by the Thomas-Fermi-Dirac (TFD) potential.[25,26] The Sarafyan-Butcher embedding formula[27] was used for integration of Eq. (4). The integration procedure was continued until the radius r_0 of the TFD potential was reached.[25] However, the function $\delta_l(r)$ was becoming practically constant much earlier. Up to 80 phase shifts were necessary to obtain sufficient accuracy of Eq. (3). The above algorithm requires a computer with wide range of constants, i.e., $10^{\pm300}$. It can be run using a FORTRAN 77 compiler on an IBM PC.

D. Relativistic approach

For the sake of completeness, the relativistic elastic cross sections were calculated using a method similar to that of Ichimura *et al.*[13] As was shown by Lin *et al.*,[28] the elastic scattering problem is reduced to solution of a differential equation of the form

$$\frac{d\phi^{\pm}}{dr}=\frac{k}{r}\sin(2\phi^{\pm})+[W-V(r)]-\cos(2\phi^{\pm}) , \tag{5}$$

where W is the total energy of the electron, $k=-(l+1)$ for the "spin-up" case $(+)$, and $k=l$ for the "spin-down" case $(-)$. The energy is in units of $mc^2=511\,004.06$ eV and the length r is in units of $\hbar/(mc)=0.003\,861\,6$ Å. The phase shifts $\delta_l^{\pm}$ are calculated from

$$\tan\delta_l^{\pm}=\frac{Kj_{l+1}(Kr)-j_l(Kr)[(W+1)\tan\phi_l^{\pm}+(1+l+k)/r]}{Kn_{l+1}(Kr)-n_l(Kr)[(W+1)\tan\phi_l^{\pm}+(1+l+k)/r]} ,$$

where $K^2=W^2-1$, $j_l(Kr)$ and $n_l(Kr)$ are the spherical Bessel functions, and

$$\phi_l^{\pm}=\lim_{r\rightarrow\infty}\phi_l^{\pm}(r) .$$

In this work Eq. (5) was solved numerically using the fifth-order Runge-Kutta algorithm (Nyström formula, Ref. 27, p. 50). The starting value of $\phi_l^{\pm}(r)$ for small r was found by expansion of the potential into a series of the form

$$V(r)=-\frac{1}{r}(Z_0+Z_1r+Z_2r^2+\cdots) .$$

The expansion coefficients Z_0, Z_1, Z_2, etc. were calculated from the analytical fit of $V(r)$ given by Bonham and Strand.[26] Calculations for all l were carried out starting at $r=0.05$ ($=0.000\,193$ Å) with an integration step of $h=0.025$. Particular care should be taken in calculations of the function $j_l(Kr)$. Eventually, the differential elastic cross sections were calculated from (Ref. 23, p. 228)

$$d\sigma/d\Omega=|f(\theta)|^2+|g(\theta)|^2 , \tag{6}$$

where

$$f(\theta)=\frac{1}{2iK}\sum_l \{(l+1)[\exp(2i\delta_l^+)-1] + l[\exp(2i\delta_l^-)-1]\}P_l(\cos\theta) ,$$

$$g(\theta)=\frac{1}{2iK}\sum_l [\exp(2i\delta_l^-)-\exp(2i\delta_l^+)]P_l^1(\cos\theta) ,$$

where

$$P_l^1(z)=(1-z^2)^{1/2}\frac{dP_l(z)}{dz} .$$

The energy dependencies of the total scattering cross sections calculated by integrating Eqs. (3) and (6) are practically identical with those calculated by Ichimura and Shimizu.[14] The corresponding elastic mean free path λ_θ for the considered elements varies between 4 and 30 Å at energies in the range 300–2400 eV.

III. EXPERIMENTAL PROCEDURE

A four-grid retarding field electron energy analyzer with an acceptance angle of 3.5° was constructed. The plane circular stainless-steel grids were fixed by ceramic rings in a stainless-steel tube (see Fig. 1). The analyzer was mounted on a manipulator in a ultrahigh-vacuum (UHV) chamber with a base pressure below 10^{-10} Torr and could be rotated with respect to the sample. The sample was placed on the rotational axis of the analyzer at normal to the incoming electron beam. The angle of the analyzer with respect to the surface normal could then be adjusted externally by rotating the manipulator.

Experiments were performed on a polycrystalline Pd sample and on a Si(111) single crystal which was bombarded with 5 keV Ar^+ ions to destroy the crystallinity of the sample. The samples were sputter cleaned by a standard procedure which was previously found to produce samples with a surface contamination below 1%. Reflection electron energy-loss spectra (REELS) were recorded under variation of the primary electron energy and the angle from the surface normal to the analyzer. In each case, the analyzer axis was adjusted to give the maximum height and minimum width of the elastic peak. The peak shape was observed to be unchanged under variation of the angle of analysis. Therefore, relative areas of the elastic peak could be determined by consistent use of a well-defined part of the peak, which was sufficiently narrow not to include inelastically scattered electrons.

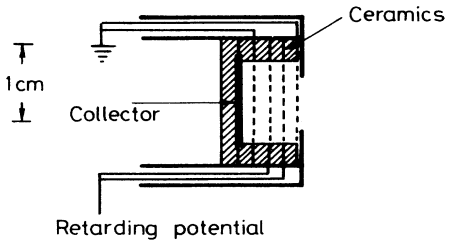

FIG. 1. Schematic diagram of the analyzer.

IV. RESULTS

A. Comparison of elastic scattering cross sections

The present calculations of the elastic scattering cross sections were performed in the energy range 200–3000 eV for elements with atomic number varying between 13 and 79. Exemplary angular dependences of the differential scattering cross sections are shown in Figs. 2(a)–2(d). As one can see, the first-order Born approximation (FBA) provides erroneous results from medium- and high-atomic-number elements. The total scattering cross section is overestimated by about 1 order of magnitude. These effects are much more pronounced below 1000 eV. Similar conclusions were reported by Ichimura *et al.*[13] and Ichimura and Shimizu,[14] who compared the relativistic PWEM scattering cross sections with the screened Rutherford and the FBA cross sections. Thus the partial-wave expansion method must be used for calculating the elastic backscattering probabilities at the energies considered here.

The relativistic and nonrelativistic cross sections are practically identical for low- and medium-atomic-number elements. A noticeable difference is observed for gold. This effect, found for higher-atomic-number elements will be a subject of a separate study.

It has been decided that the theoretical and experimental investigations reported in this work are limited to the elements with low and medium atomic numbers. All the calculations of the backscattering probabilities reported in the following sections were made within the nonrelativistic approach.

B. Angular distribution of elastically backscattered electrons

The elastically backscattered intensities were measured for silicon and palladium by the analyzer shown in Fig. 1. The experimental results are shown in Fig. 3 for exit angles $\alpha=45°$ and 75° with respect to the surface normal and for energies between 300 and 1200 eV. For each of the primary energies, the area of the elastic peak has been normalized to the peak area recorded at $\alpha=15°$. The thin solid lines through the experimental points are to guide the eye. The intensity of backscattered electrons depends on both the solid and the primary electron energy. Thus, for both solids, the relative elastic intensity is higher for $\alpha=45°$ than for $\alpha=75°$, whereas the intensity varies unsystematically with the electron energy.

Within the P_1 approximation, Eq. (1) is valid. Since

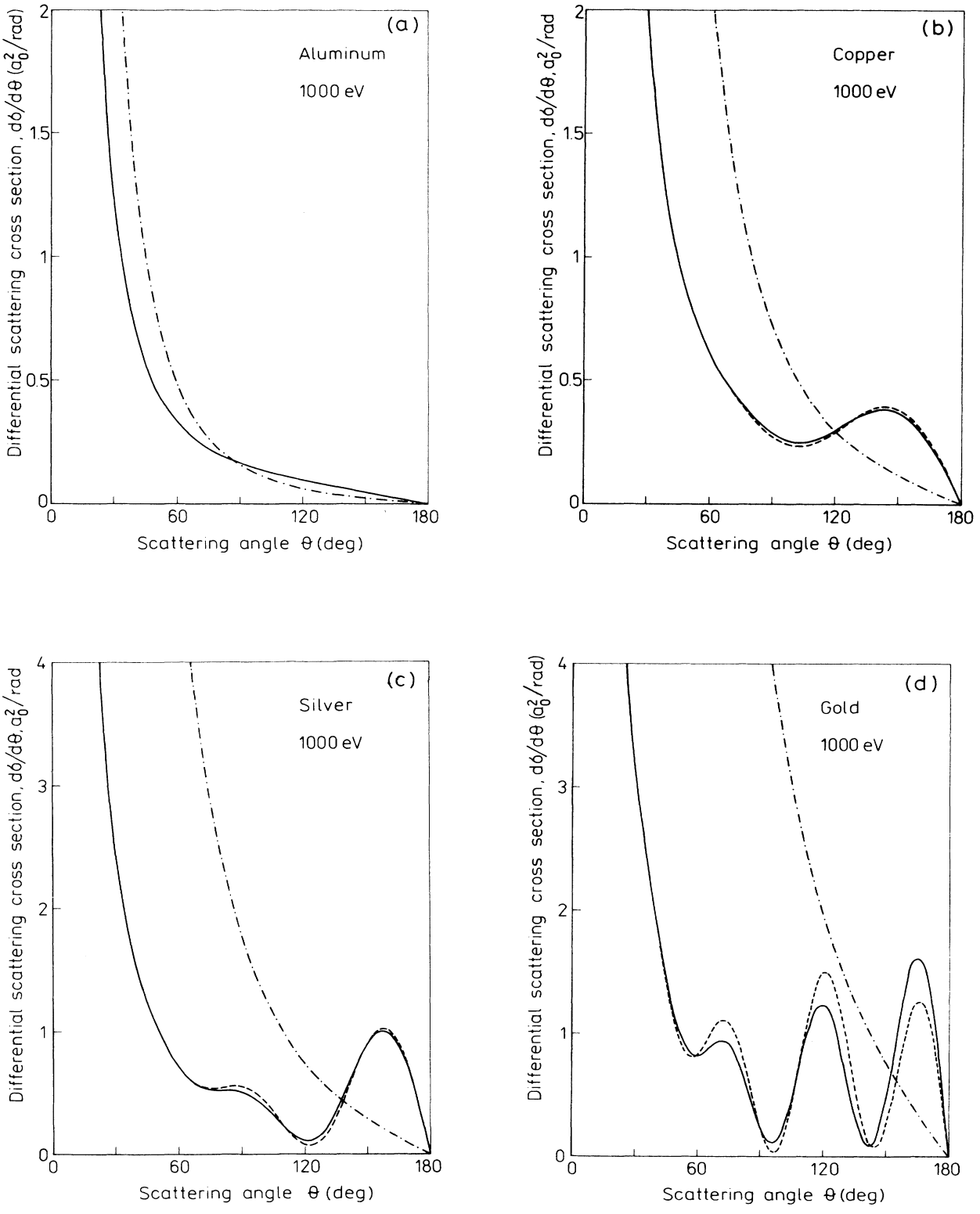

FIG. 2. Angular dependence of the differential scattering cross section, $d\sigma/d\theta = 2\pi(d\sigma/d\Omega)\sin\theta$ at energy 1000 eV. Solid line, nonrelativistic approach; dashed line, relativistic approach; dot-dashed line, first-order Born approximation. (a) Aluminum, (b) copper, (c) silver, and (d) gold.

the dependence on atomic number and energy only enters through the factor containing λ_1 and λ, it follows that the flux of elastically backscattered electrons relative to the flux at $\alpha=15°$ is independent of both primary energy and atomic number. Thus

$$J_l(\alpha) \propto \cos\alpha + 3/2\cos^2\alpha \ .$$

The ratio $J_l(\alpha)/J_l(15°)$ is also shown in Fig. 3 (thick solid lines) for $\alpha=45°$ and 75°. It is evident that although the P_1 approximation does account for the general trend in the experimental data as α is varied, it does fail to describe the detailed variation. Thus the experimentally observed intensity depends strongly on both the element as well as the energy. This is not predicted by the P_1 approximation which deviates by up to a factor of 4 from experiment.

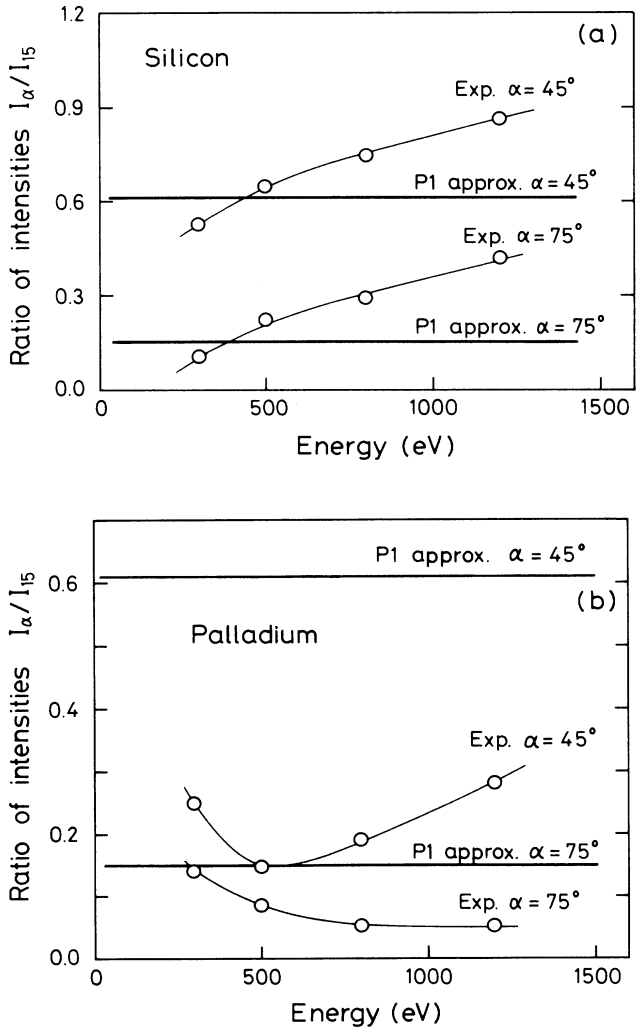

FIG. 3. Energy dependence of the elastically backscattered intensity at different exit angles α towards the surface normal. Circles, experimental values for (a) silicon and (b) palladium. Thin solid lines are to guide the eye through the experimental points. Thick solid lines, P_1 approximation. All data are normalized to the intensity at $\alpha=15°$.

The angular distribution of electrons elastically backscattered from silicon and palladium was then calculated using the proposed Monte Carlo algorithm. The input parameters for the Monte Carlo calculations are the parameters specifying the geometry of the experiment, the elastic scattering cross sections, and the inelastic mean free path of electrons. In the present calculations, it has been decided to use the values of IMFP resulting from theoretical calculations, since the usual experimental methods provide actually projections of IMFP on the direction of analysis.[29] Thus, the input values of IMFP were taken from papers by Penn[30] and Ashley and Tung.[31]

It turned out that, indeed, the angular distribution of elastically backscattered electrons could not be described with one universal curve. Histograms of the angular distribution of 500-eV electrons backscattered from silicon and palladium are shown in Fig. 4. Both histograms are also normalized to unity at $\alpha=15°$. As one can see, much better agreement between the calculated histograms and the experimental data is observed than in the case of the P_1 approximation. Good agreement is also observed at other energies. Figures 5(a) and 5(b) show the energy dependence of the elastically backscattered intensity at $\alpha=45°$ and 75°. The shape of the experimental dependence is closely reproduced. The experimental intensities measured for silicon are somewhat overestimated by theory. However, this effect can be due to an error in the input values of the IMFP, since these values are known

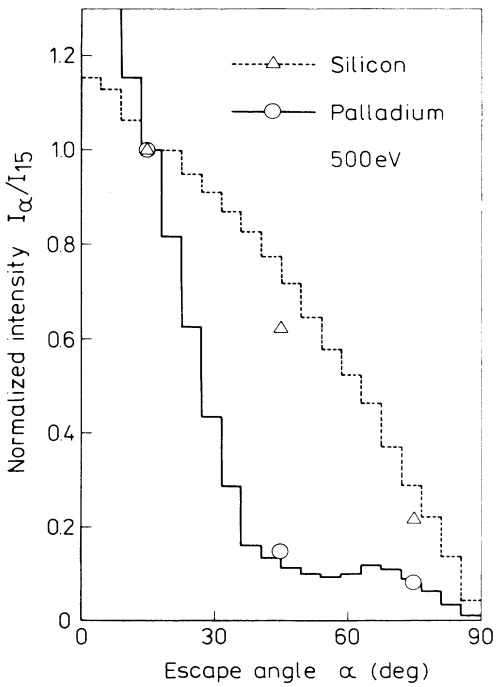

FIG. 4. Comparison of the Monte Carlo calculated angular distribution of elastically backscattered electrons at energy 500 eV with experimental intensities. Solid histograms are the theoretical values. Circles and triangles are the experimental values for palladium and silicon, respectively. All data are normalized with respect to the intensity at $\alpha=15°$.

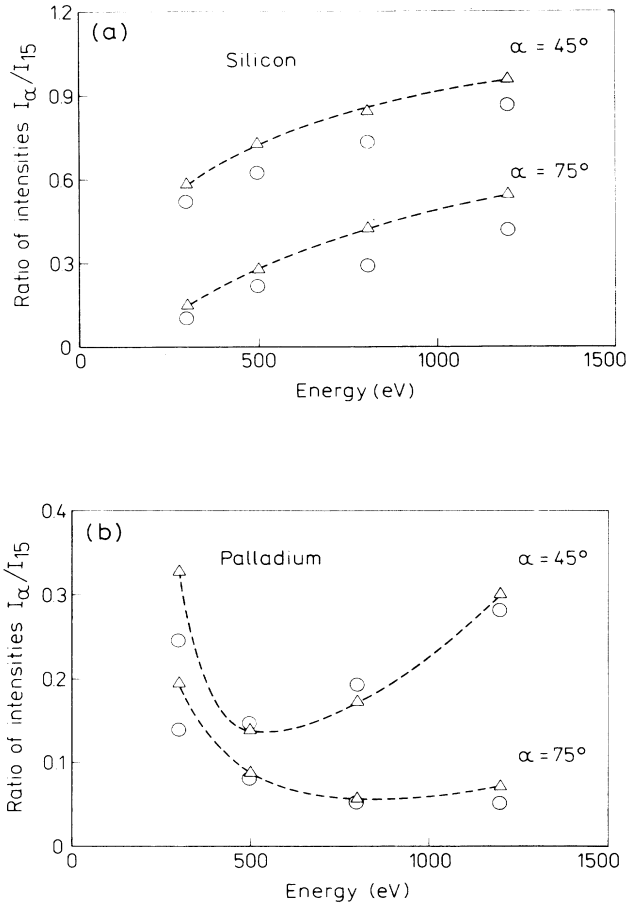

FIG. 5. Energy dependence of the elastically backscattered intensity at different angles α towards the surface normal. Circles, experimental values; triangles, Monte Carlo calculations. (a) Silicon and (b) palladium. All data are normalized with respect to the intensity at $\alpha=15°$.

with relatively poor accuracy.

The excellent agreement obtained between theory and experiment, in Figs. 4 and 5, has stimulated the present authors to perform the Monte Carlo calculations of the angular distributions for systems studied experimentally by other authors. The histograms for Al, Cu, and Ag resulting from the present calculations at 400 and 1000 eV electron energy are shown in Figs. 6(a)–6(f). Also shown are the distributions determined experimentally by Bronshtein and Pronin.[9] Note the excellent agreement between theory and experiment in all cases shown. Similar agreement was obtained at other energies. Slightly larger differences were observed at 200 eV energy, which may be due to the fact that the depth of electron penetration is rather low and elastic backscattering of electrons may be influenced by surface contaminations and surface roughness. Also at low energies the Poisson process approximation may also become less valid. All the histograms and all the experimental distributions were normalized to the intensity measured at $\alpha=25°$. One can notice that the shape of the histograms is practically the same for values of IMFP taken from Penn[30] and from Ashley and Tung,[31] despite the fact that they differ considerably in some cases (e.g., by $\sim 30\%$ in the case of Cu).

C. Energy dependence of elastic backscattering probabilities

Bronshtein and Pronin[9] published the energy dependence of the elastically backscattered intensity measured in the energy range 100–2000 eV for several elements in the direction at $\alpha=25°$ towards the surface normal. The experimental plots of intensity versus energy exhibited maxima for medium-atomic-number elements (see Fig. 7, solid lines). The algorithm proposed in the present work was used to calculate the elastically backscattered intensity in the same direction. The results are compared with the experimental data in Figs. 7(a)–7(c). The data of Bronshtein and Pronin were published in arbitrary units. The same scaling factor was used to the calculated intensities resulting from the IMFP published by Penn[30] or Ashley and Tung,[31] and this accounts for the observed scatter. The shape of the experimental and the theoretical dependences is practically the same. Also the theory predicts very accurately the position of the maximum.

Schmid *et al.*[10] reported extensive experimental data on the reflection probability in a well-defined solid angle, i.e., within the solid angle of the retarding field analyzer (from $\alpha=6°$ to 52°). Experiments were performed in the energy range 60–2500 eV. In the present work the calculations of the reflection probability were performed for the same solid angle. Results are shown in Figs. 8(a)–8(c). Again, a very good agreement is observed between the experimental and theoretical energy dependences. Note that in this case, however, we compare the *absolute values* of the probabilities. The observed agreement is thus a very convincing proof for the validity of the presented theory.

Bronshtein and Pronin[9] and Schmid *et al.*[10] noticed that the position of a maximum on energy dependences shifts toward higher energies with increasing atomic number. These authors did not attempt to explain the observed effect. The energy dependences calculated in the present work also exhibit the shift of the maximum. This can be obviously attributed to the corresponding behavior of the elastic scattering cross sections.

V. DISCUSSION

It is evident from Fig. 3 that the P_1 approximation very roughly accounts for the general behavior of the angular distribution of the elastically backscattered intensity. However, it completely fails to describe the detailed variation of the observed intensity for a given energy and element. The differential elastic scattering cross sections exhibit a strong resemblance to the experimental angular distribution of elastically backscattered electrons. In particular, in both cases we observe the presence of minima and maxima. This shows that the region of the elastic peak in the energy spectra is dominated by a single large-angle elastic scattering event. The P_1 approximation is expected to be insufficient when an electron has

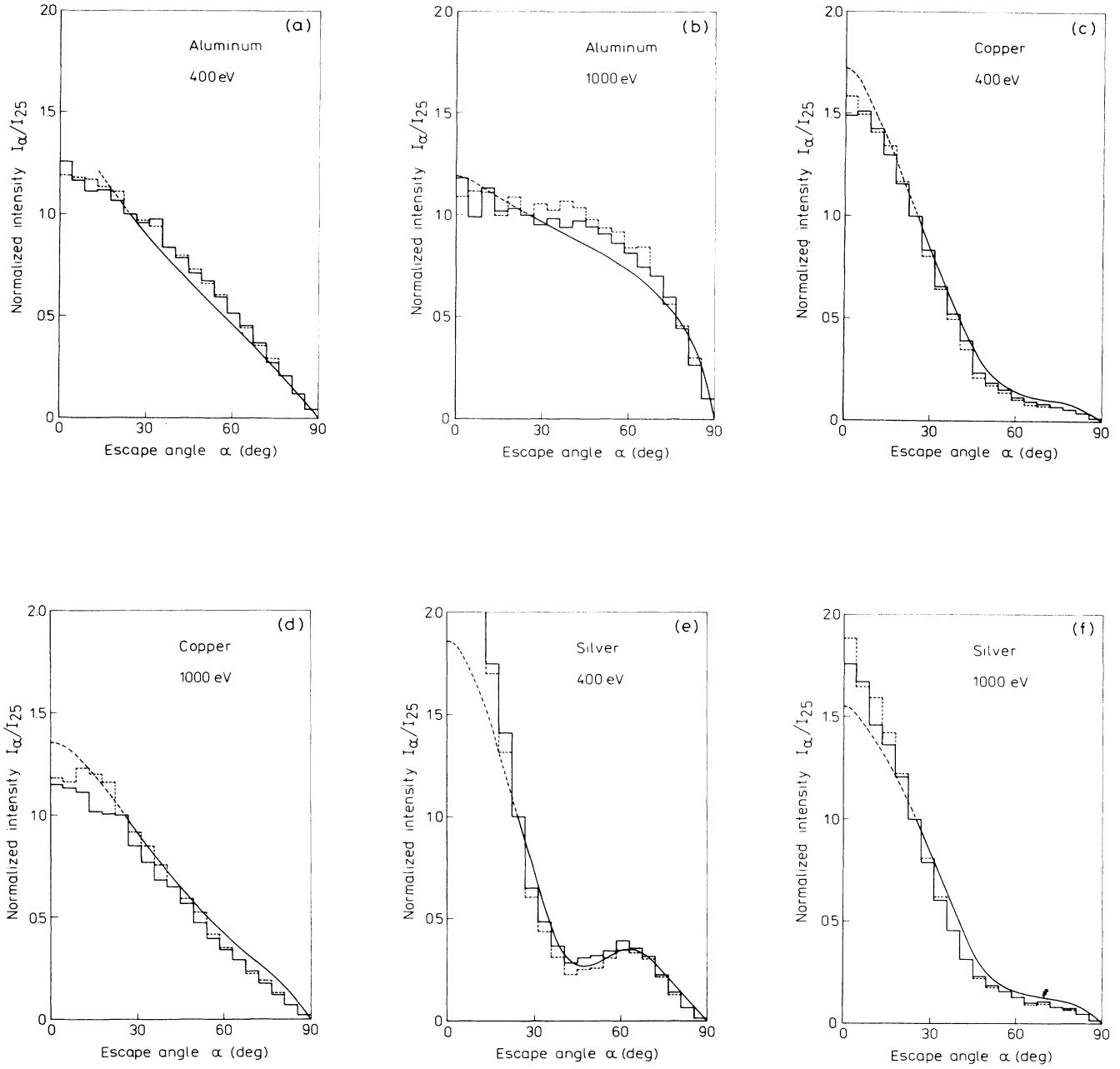

FIG. 6. Comparison of the calculated and experimental angular distributions of elastically backscattered electrons. Solid histogram, the input IMFP values taken from Ashley and Tung (Ref. 31); dashed histogram, the input IMFP values taken from Penn (Ref. 30); solid line, experimental distribution of Bronshtein and Pronin (Ref. 9). (a) Aluminum 400 eV, (b) aluminum 1000 eV, (c) copper 400 eV, (d) copper 1000 eV, (e) silver 400 ev, and (f) silver 1000 eV. All distributions are normalized with respect to the intensity at $\alpha = 25°$.

undergone a few scattering events, and this explains the failure to describe the elastic backscattering from surfaces.

The Monte Carlo algorithm based on theoretical elastic scattering cross sections is proved to be a powerful tool for predicting the characteristics of elastic backscattering. An excellent agreement is observed between the theoretical prediction and the experimental data arising from three different laboratories. This agreement cannot be fortuitous. In an earlier paper an attempt has been made to describe the elastic backscattering within the first-order Born approximation.[4] It turned out that the FBA provides reasonable results for low- and medium-atomic-number elements at energies exceeding 2000 eV. The limit of validity seems to be much lower when the elastic scattering cross sections are calculated within

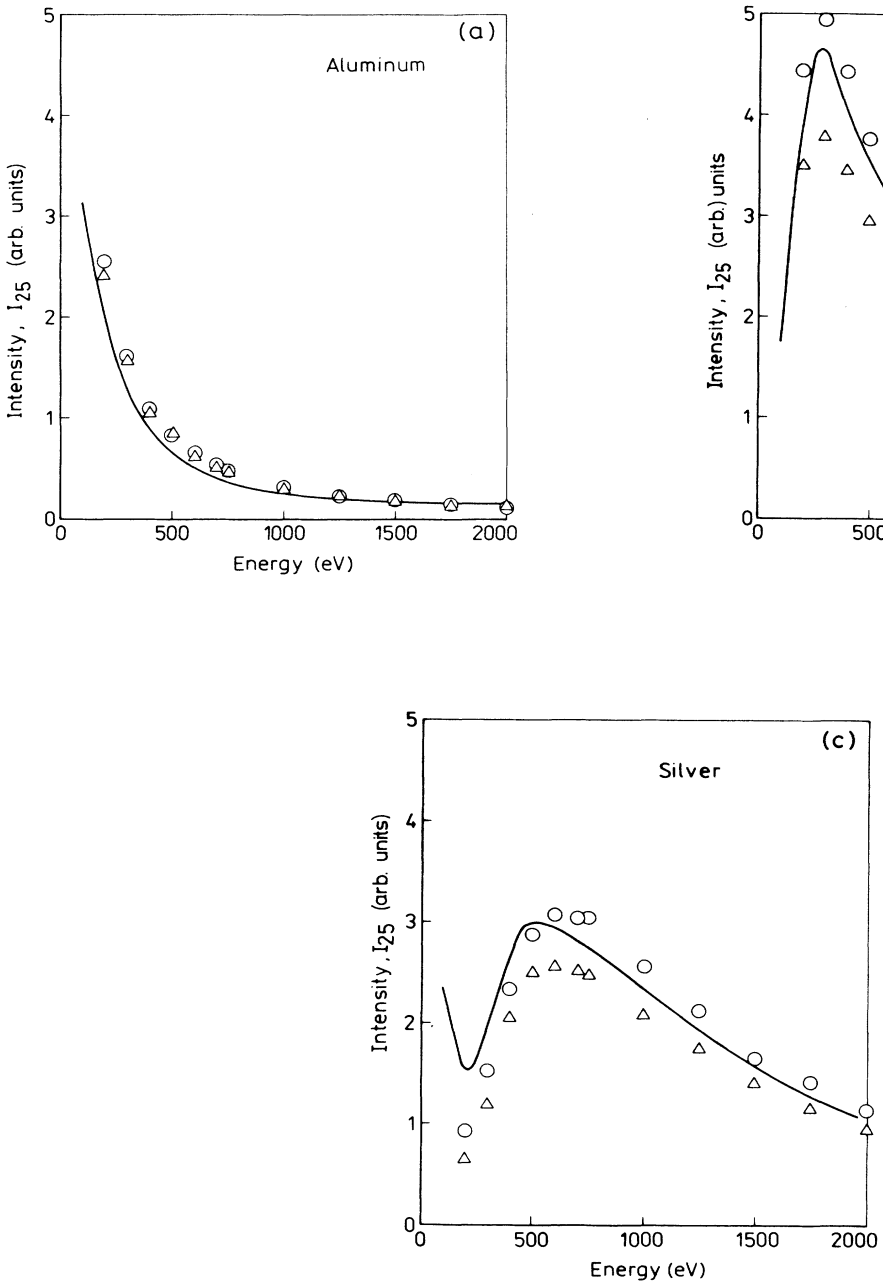

FIG. 7. Energy dependence of the elastically backscattered intensity. Solid line, experimental dependence taken from Bronshtein and Pronin (Ref. 9); circles, calculated values, the IMFP taken from Ashley and Tung (Ref. 31); triangles, calculated values, the IMFP taken from Penn (Ref. 30). (a) Aluminum, (b) copper, and (c) silver.

PWEM. Comparison of the results of calculations with the experimental data shows that 200 eV can be assumed as a lower limit of validity. At lower energies different theoretical models should be applied. Probably the interaction of an electron with several neighboring scattering centers should be considered rather than a series of collisions of a given electron with single scattering centers. However, the former model involves considerable computational difficulties.

The Thomas-Fermi-Dirac potential is found to describe adequately the scattering centers of a solid in the energy range considered in the present work. In fact, this potential was extensively used in elastic scattering calculations.[4,11,12] Ichimura and Schimizu compared, in the energy range up to 20 keV, the total scattering cross sections for aluminum resulting from Hartree-Fock (HF) and TFD potentials. They were found to be practically identical. In principle, it would be possible to perform

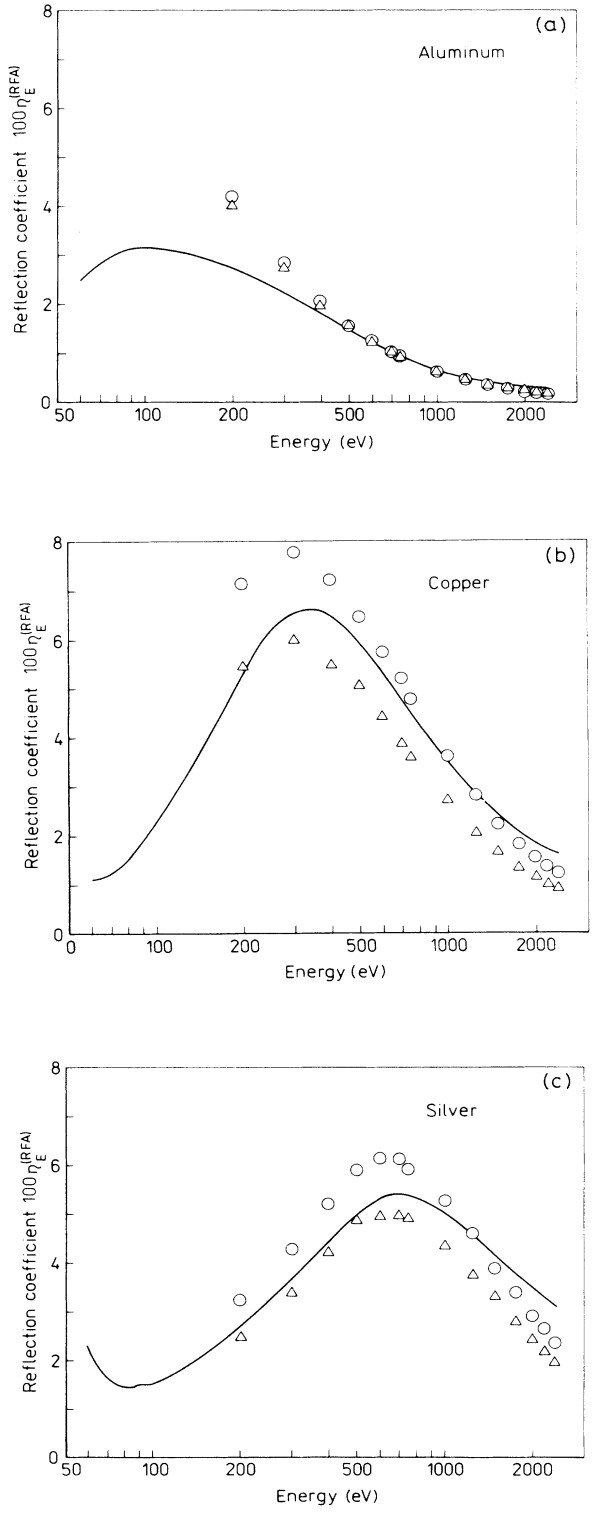

FIG. 8. Energy dependence of the reflection probability into the solid angle of the retarding filed analyzer (RFA). Solid line, experimental dependence taken from Schmid *et al.* (Ref. 10); circles, calculated values, the IMFP taken from Ashley and Tung (Ref. 31); triangles, calculated values, the IMFP taken from Penn (Ref. 30).

calculations of elastic scattering cross sections within the PWEM using published data on HF potentials.[32,33] Such calculations, however, would be much more complicated. Furthermore, the published HF potentials cover only a limited range of atomic numbers.

The differential elastic scattering cross sections calculated in the present work may not be reliable at small scattering angles since the TFD potential has a truncation point.[25] On the other hand, the small-angle collisions have negligible effect on the electron trajectory, particularly when the phenomenon of elastic backscattering is dominated by a single large-angle collision.

Figures 7 and 8 indicate that the calculated reflection probabilities depend considerably on the input values of the IMFP. The calculated probabilities can easily be adjusted to the experimental values by the proper choice of the input value of the IMFP. Such a procedure would provide the values of IMFP in a wide energy range. Actually, the values of IMFP are usually known with poor accuracy, and a suggestion has already been made to determine the IMFP from the measured elastic backscattering intensities.[4] However, the theoretical models involved in published calculations have not been as accurate as those in the present work.

In conclusion, the elastic backscattering of electrons from surfaces at energies relevant for surface electron spectroscopies can be surprisingly well described by the multiple elastic scattering model based on differential elastic scattering cross sections resulting from the PWEM. This theoretical model is not universal and has two limitations. Firstly, it requires a considerable amount of computer time. The calculations associated with scattering cross sections can be run on an IBM PC. However, the access to a large computer is recommended when performing the Monte Carlo simulations. Secondly, the theory is applicable to polycrystalline or amorphous solids, since the diffraction effects are neglected. Description of the electron trajectory by the Poisson process involves an assumption of random positions of scattering centers in a solid.

ACKNOWLEDGMENT

Two of the authors (A.J. and J.G.) would like to acknowledge the support of the Research Projects CPBR 12.2.84 and 3.20.81.

APPENDIX

The Riccati-Bessel functions exhibit the following behavior near the origin (Ref. 24, p. 199):

$$\hat{j}_l(x)\rightarrow\frac{x^l}{(2l+1)!!}\ ,\qquad \hat{n}_l(x)\rightarrow-(2l-1)!!x^{-1}\ . \tag{A1}$$

Suppose that the scattering potential $V(r)$ is approximated by the function V_0r^{-m} for small values of r. We have (Ref. 24, Chap. 3)

$$\delta_l(r)=-\frac{1}{K^2}\frac{2m}{\hbar^2}V_0\frac{(Kr)^{2l+3}}{[(2l-1)!!]^2(2l+3-m)}\ . \tag{A2}$$

From Eqs. (A1) and (A2) we obtain for $r \to 0$

$$\sin\delta_l(r)\hat{n}_l(r) \to \frac{1}{K^2}\frac{2m}{\hbar^2}V_0\frac{(2l-1)!!K^{l+2}r^{l+3-m}}{[(2l+1)!!]^2(2l+3-m)} ,$$

$$\cos\delta_l(r)\hat{j}_l(r) \to \frac{K^{l+2}}{(2l+1)!!}r^{l+1} .$$

Thus the relation

$$\hat{j}(Kr)\cos\delta_l(r) \gg \hat{n}_l(Kr)\sin\delta_l(r)$$

is valid if $m < 2$. For the TFD potential we have $V_0 = -Ze^2$ and $m = 1$.

[1]J. Pavluch and L. Eckertova, Surf. Sci. **162**, 896 (1985).
[2]G. Gergely, Surf. Interface Anal. **3**, 201 (1981).
[3]G. Gergely, Vacuum **33**, 89 (1983); **37**, 149 (1987); Scanning **8**, 203 (1986).
[4]A. Jablonski, Surf. Sci. **151**, 166 (1985).
[5]J. S. Schilling and M. B. Webb, Phys. Rev. B **2**, 1665 (1970).
[6]W. Dietzel, G. Meister, and E. Bauer, Z. Phys. B **47**, 189 (1982).
[7]T. Oguri, H. Ishioka, H. Fukuda, and M. Irako, J. Phys. Soc. Jpn. **55**, 414 (1986).
[8]I. M. Bronshtein, V. P. Pronin, and V. M. Stozharov, Fiz. Tverd. Tela (Leningrad) **16**, 2107 (1974) [Sov. Phys.—Solid State **16**, 1374 (1975)].
[9]I. M. Bronshtein and V. P. Pronin, Fiz. Tverd. Tela (Leningrad) **17**, 2086 (1975) [Sov. Phys.—Solid State **17**, 1363 (1976)].
[10]R. Schmid, K. H. Gaukler, and H. Seiler, in *Scanning Electron Microscopy/1983,* edited by O. Johari (SEM, AMF O'Hare, IL, 1983), Vol. II, p. 501.
[11]A. L. Tofterup, Phys. Rev. B **32**, 2808 (1985).
[12]S. Goudsmit and J. L. Saunderson, Phys. Rev. **57**, 241 (1940).
[13]S. Ichimura, M. Aratama, and R. Schimuizu, J. Appl. Phys. **51**, 2853 (1980).
[14]S. Ichimura and R. Schimizu, Surf. Sci. **112**, 386 (1981); R. Schimizu and S. Ichimura, Toyota Foundation Technical Report No. I-006, 76-0175, 1980 (unpublished).
[15]R. Schimizu, Y. Kataoka, T. Ikuta, T. Koshikawa, and H. Hashimoto, J. Phys. D **9**, 101 (1976).
[16]F. Salvat and J. Parellada, J. Phys. D **17**, 185 (1984).
[17]M. Fink and A. C. Yates, At. Data Nucl. Data Tables **1**, 385 (1970).
[18]M. Fink and J. Ingram, At. Data Nucl. Data Tables **4**, 129 (1972).
[19]D. Gregory and M. Fink, At. Data Nucl. Data Tables **14**, 39 (1974).
[20]M. E. Riley, C. J. MacCallum, and F. Biggs, At. Data. Nucl. Data Tables **15**, 443 (1975).
[21]L. Reimer and B. Lödding, Scanning **6**, 128 (1984).
[22]T.-Y. Wu and T. Ohmura, *Quantum Theory of Scattering* (Prentice Hall, Englewood Cliffs, 1962), p. 6.
[23]N. F. Mott and H. S. W. Massey, *The Theory of Atomic Collisions* (Clarendon, Oxford, 1965), p. 24.
[24]F. Calogero, *Variable Phase Approach to Potential Scattering* (Academic, New York, 1967).
[25]L. H. Thomas, J. Chem. Phys. **22**, 1758 (1954).
[26]R. A. Bonham and T. G. Strand, J. Chem. Phys. **39**, 2200 (1963).
[27]L. Lapidus and J. H. Seinfeld, *Numerical Solution of Ordinary Differential Equations* (Academic, New York, 1971), p. 72.
[28]S. R. Lin, N. Sharman, and J. K. Percus, Nucl. Phys. **45**, 492 (1963).
[29]C. J. Powell, J. Vac. Sci. Technol. A **3**, 1338 (1985).
[30]D. R. Penn, J. Electron Spectrosc. Relat. Phenom. **9**, 29 (1976).
[31]J. C. Ashley and C. J. Tung, Surf. Interface Anal. **4**, 52 (1982).
[32]R. G. Strand and R. A. Bonham, J. Chem. Phys. **40**, 1686 (1964).
[33]E. Clementi and C. Roetti, At. Data Nucl. Data Tables **14**, 177 (1974).